

The entropy distribution in clusters: evidence of feedback?

Scott T. Kay^{*}

Department of Physics and Astronomy, University of Sussex, Falmer, Brighton BN1 9QJ

2 February 2008

ABSTRACT

The entropy of the intracluster medium at large radii has been shown recently to deviate from the self-similar scaling with temperature. Using N -body/hydrodynamic simulations of the Λ CDM cosmology, we demonstrate that this deviation is evidence that feedback processes are important in generating excess entropy in clusters. While radiative cooling increases the entropy of intracluster gas, resulting in a good match to the data in the centres of clusters, it produces an entropy-temperature relation closer to the self-similar scaling at larger radii. A model that includes feedback from galaxies, however, not only stabilises the cooling rate in the simulation, but is capable of reproducing the observed scaling behaviour both in cluster cores and at large radii. Feedback modifies the entropy distribution in clusters due to its increasing ability at expelling gas from haloes with decreasing mass. The strength of the feedback required, as suggested from our simulations, is consistent with supernova energetics, providing a large fraction of the energy reaches low-density regions and is originally contained within a small mass of gas.

Key words: methods: N -body simulations – hydrodynamics – X-rays: galaxies: clusters – galaxies: clusters: general

1 INTRODUCTION

Entropy¹ has become the standard quantity for describing the distribution of the intracluster medium. In a self-similar population of clusters, where entropy originates solely due to gravitational infall via shock-heating, entropy scales proportional to the system's virial temperature, $S \propto T_{\text{vir}}$. Such a model, however, does not reproduce the observed X-ray properties of groups and clusters. The most striking example of this failure is the X-ray luminosity-temperature ($L_X - T_X$) relation: the self-similar scaling, $L_X \propto T_X^\alpha$, where $\alpha = 2$ (Kaiser 1986) is flatter than the observed relation for clusters, $\alpha \sim 3$ (e.g. Edge & Stewart 1991; Mushotzky & Scharf 1997).

This deficit in luminosity, primarily in low-mass systems, is due to an excess of entropy in cluster cores (Evrard & Henry 1991; Kaiser 1991), a phenomenon first measured by Ponman, Cannon & Navarro (1999). Understanding the origin of this entropy is central to our understanding of cluster physics (Bower 1997; Voit et al. 2002, 2003). Directly heating the intracluster gas is the most common solution to this problem, however a variety of theoretical studies conclude that the obvious candidates – supernovae – are at best only marginally capable of generating the required excess en-

trophy (e.g. Balogh, Babul & Patton 1999; Kravtsov & Yepes 2000; Loewenstein 2000; Wu, Fabian & Nulsen 2000; Bower et al. 2001; Borgani et al. 2002). More energetic forms of supernovae (so-called hypernovae) may be important. Alternative sources of energy that are clearly observed to be interacting with the intracluster medium are Active Galactic Nuclei (AGN), capable of distributed heating through their release of bubbles and jets (e.g. Quilis, Bower & Balogh 2001; Brüggen & Kaiser 2002; Omma et al. 2003).

Recently, attention has also focused on the effects of radiative cooling, which selectively removes the low-entropy material to form galaxies, causing higher-entropy material to flow in to replace it (Knight & Ponman 1997; Pearce et al. 2000; Bryan 2000; Muanwong et al. 2001, 2002; Davé, Katz & Weinberg 2002; Wu & Xue 2002). Cooling is an appealing mechanism as it involves no free parameters (other than the metallicity of the gas, which is observable): the observed level of excess entropy is consistent with the removal of low-entropy gas with cooling times shorter than the age of the Universe, scaling as $S \propto T^{2/3}$ (Voit & Bryan 2001). Cooling, if unchecked however, overproduces the mass in galaxies, requiring a feedback mechanism in order to regulate itself (White & Rees 1978; Cole 1991; Balogh et al. 2001), but as was pointed out by Voit & Bryan (2001), their argument still holds so long as feedback efficiently transports cold gas away from cluster cores.

Perhaps the likely source of excess entropy is from a combination of cooling and heating processes (Kay, Thomas

^{*} E-mail: s.t.kay@sussex.ac.uk

¹ We define entropy as $S = kT/n_e \gamma^{-1}$ keV cm², where $\gamma = 5/3$ is the ratio of specific heats for a monatomic ideal gas.

& Theuns 2003; Tornatore et al. 2003). For example, Kay et al. (2003) studied the combined effects of cooling and feedback (by reheating cold galactic gas) in simulations of groups and concluded that feedback, as well as regulating cooling, could contribute to the excess core entropy in systems with virial temperatures smaller than the heating temperature. In larger systems where this temperature inequality was reversed, the inability of reheated gas to escape from the halo reduces the average entropy of the gas, and if the heating temperature is low enough, will affect the core entropy.

Attention has now shifted to observing the entropy of intracluster gas at larger radii. In a recent paper, Ponman, Sanderson & Finoguenov (2003) measured the entropy-temperature relation at a significant fraction of the virial radius (R_{500}) for a sample of 66 galaxies, groups and clusters: the Birmingham-CfA Cluster Scaling Project (see also Sanderson et al. 2003; Sanderson & Ponman 2003). In their study, they measured the same deviation from self-similarity ($S \propto T^{2/3}$) already observed in the core. This scaling behaviour was also verified recently by Pratt & Arnaud (2003), using *XMM-Newton* observations of Abell 1413 & 1983. In this paper, we will argue that these observations are evidence that feedback plays a significant role in forming the entropy distribution in clusters.

The rest of this paper is organized as follows. In Section 2 we describe the simulations used to perform this study. Our results are presented in Section 3 and summarized in Section 4.

2 METHOD

2.1 Simulation details

We have performed four simulations of the Λ CDM cosmology, setting $\Omega_m = 0.3$, $\Omega_\Lambda = 0.7$, $\Omega_b = 0.045$, $h = 0.7$ & $\sigma_8 = 0.9$, consistent with the *WMAP* results. Each run started from the same initial conditions: a regular cubic mesh of 2,097,152 (128^3) particles (each of gas and dark matter) within a box of comoving length $60 h^{-1}$ Mpc. This set the gas and dark matter particle masses to be $m_{\text{gas}} \sim 1.3 \times 10^9$ and $m_{\text{CDM}} \sim 7.3 \times 10^9 h^{-1} M_\odot$ respectively. The runs were started at $z = 49$ and evolved to $z = 0$, using a gravitational softening length equal to $20 h^{-1}$ kpc in comoving co-ordinates.

The code used in this study is a parallel (MPI) version of GADGET (Springel, Yoshida & White 2001), an N -body/hydrodynamics code that uses a PM-tree to calculate gravitational forces and Smooth Particle Hydrodynamics (SPH, e.g. Monaghan 1992) to calculate gas forces. This version of GADGET uses entropy as the state variable in the time-integration of the gas (Springel & Hernquist 2002).

Differences between each of the four runs are solely due to the processes incorporated that are able to change the entropy of the gas. These details are described below.

2.1.1 Non-radiative model

In this run, gas was only able to increase its entropy through shocks. This model reproduces self-similar scalings rather well.

2.1.2 Radiative model

Gas in this model could also lose entropy through radiative processes. We implemented the isochoric approximation described in Thomas & Couchman (1992), using equilibrium cooling tables from Sutherland & Dopita (1993). We fixed the metallicity of the gas to $Z = 0.3Z_\odot$. Dense gas ($n > 10^{-3} \text{cm}^{-3}$, $\delta > 100$) which cooled below $T = 1.2 \times 10^4 \text{K}$ was converted into collisionless ‘stars’. This model significantly overproduces the mass fraction of cooled baryons (observed to be 5-10 per cent; Cole et al. 2001; Balogh et al. 2001), producing a global cooled fraction of ~ 34 per cent at $z = 0$.

2.1.3 Feedback model

To stabilize the cooling rate, we only allow some of the cooled gas to form stars and reheat the rest of the cold material. Similarly to Kay et al. (2003) we incorporate feedback effects on a probabilistic basis. (A more sophisticated heating mechanism is unwarranted for simulations of this resolution, however this method is designed to capture the gross behaviour of gas being transported out of galaxies.) Rather than instantaneously convert all cooled particles into stars, we assign a value, f_{heat} to each cooled gas particle, defined to be the fractional mass of cooled material that is reheated, and draw a random number, r , uniformly from the unit interval. If $r < f_{\text{heat}}$ then the particle is heated, otherwise it becomes collisionless. Rather than heating particles to a fixed temperature, we instead assigned them a fixed entropy, as it is this quantity that determines how far the gas can rise buoyantly out of the cluster.

We ran two simulations with feedback, hereafter referred to as *Weak Feedback* and *Strong Feedback* runs. In the former case we set $f_{\text{heat}} = 0.5$ (i.e. a cooled particle has an equal chance of forming stars or being reheated) and supply an entropy $S_{\text{heat}} = 100 \text{ keV cm}^2$ to each reheated particle. For the *Strong Feedback* simulation, we set $f_{\text{heat}} = 0.1$ and $S_{\text{heat}} = 1000 \text{ keV cm}^2$. For a cold gas particle at the same density, both runs require comparable amounts of energy per mass of collisionless material but in the *Strong Feedback* case, the energy is added to one fifth of the mass of gas in the *Weak Feedback* case.

Note that an associated temperature depends on the density of the gas. At $n = 10^{-3} \text{cm}^{-3}$ (where most of the gas is heated in the simulation) both runs require $\sim 1 \text{ keV}$ of energy per particle, comparable with the energy available from supernovae. However, cold gas within galaxies (our simulations do not resolve the internal structure of these objects) is generally at much higher densities, where much higher temperatures would be required to reach S_{heat} (if the gas flows out adiabatically). The solution to this problem is either that a large fraction of energy is transported to low-density regions in kinetic form (e.g. Strickland & Stevens 2000) or that more energetic phenomena are at work, for example hypernovae or AGN or both.

2.2 Cluster selection

Clusters in each of the simulations were selected using the method described in detail in Muanwong et al. (2002). A minimal-spanning tree is first created, of all dark matter

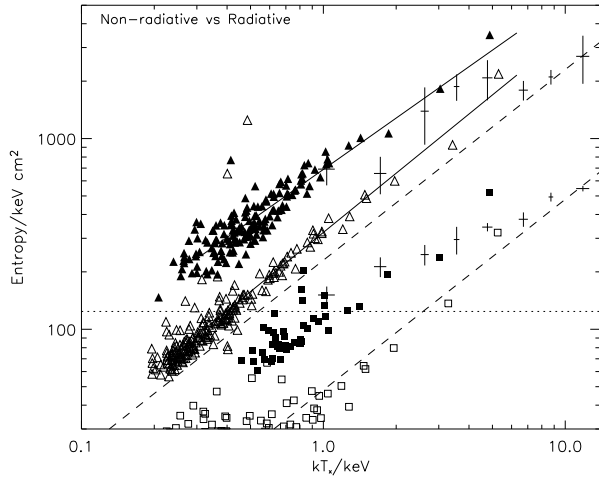


Figure 1. Entropy at fixed overdensity versus temperature for clusters in the *Non-radiative* (open symbols) and *Radiative* (filled symbols) runs at $z = 0$. Squares represent entropy values at $0.1R_{200}$ and triangles at R_{500} . Solid lines represent least-squares fits to the simulated data at R_{500} . The data-points are results from Ponman et al. (2003), with the dashed line illustrating the self-similar slope ($S \propto T$), normalized to their 8 hottest clusters. The horizontal dotted line is the entropy floor, $S \sim 124 \text{ keV cm}^2$, from Lloyd-Davies et al. (2000).

particles whose overdensity exceeds the virial value $\delta \sim 178\Omega^{-0.55}(z)$ (Eke, Navarro & Frenk 1998). The tree is then pruned using a linking length, $l = 0.5\delta^{-1/3}$ times the mean interparticle separation. Spheres are then grown around the position of maximum density in each clump of particles until the enclosed mean density (of all particles) exceeds Δ times the comoving critical density. In this paper we focus on results for $\Delta = 500$ and $\Delta = 200$. Finally, clusters with fewer than 500 particles each of baryons and dark matter are discarded.

3 RESULTS

3.1 Entropy-Temperature relation

We begin by showing results from our *Non-radiative* and *Radiative* simulations. Fig. 1 illustrates entropy at a fixed density contrast against soft-band X-ray temperature for clusters in these two runs. The temperatures are calculated as

$$T_X = \frac{\sum_i m_i \rho_i \Lambda_{\text{soft}}(T_i, Z) T_i}{\sum_i m_i \rho_i \Lambda_{\text{soft}}(T_i, Z)}, \quad (1)$$

where m_i , ρ_i and T_i are the mass, density and temperature of hot gas particle i ($T_i > 10^5 \text{ K}$) and $Z = 0.3Z_\odot$. We adopt the soft-band cooling function, Λ_{soft} , from Raymond & Smith (1977) for an energy range 0.3–1.5 keV. We calculate a mass-weighted entropy for each cluster by averaging the entropy of hot gas particles within a shell of width $20 h^{-1} \text{ kpc}$ (our results are insensitive to changing the size of this shell by a factor of 2), centred on the radius of interest.

Squares in the figure represent entropy values at $0.1R_{200}$, a radius typically chosen to highlight excess entropy

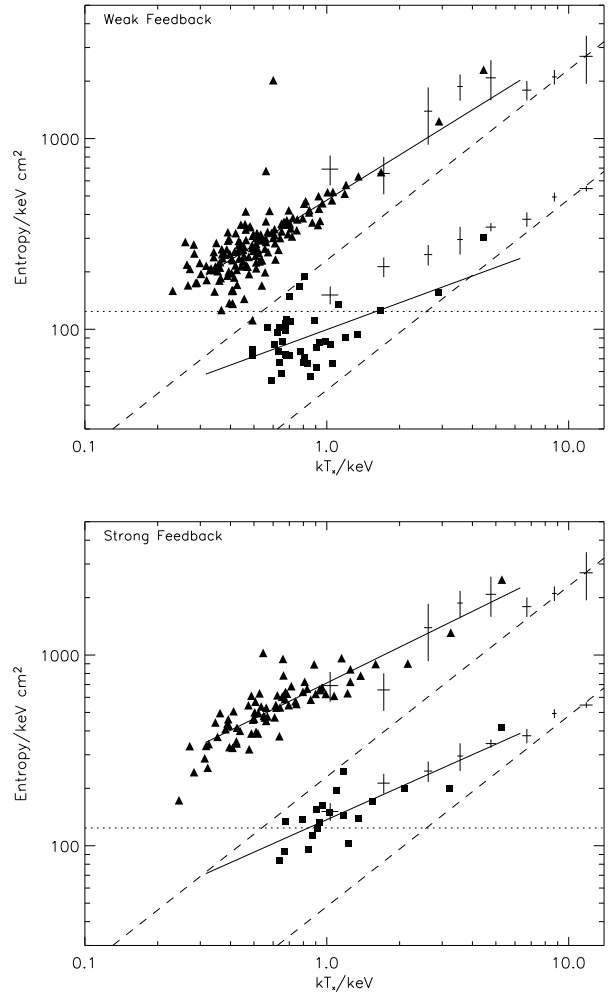


Figure 2. Entropy at fixed overdensity versus temperature for clusters in the *Weak Feedback* (top panel) and *Strong Feedback* (bottom panel) runs at $z = 0$. Squares represent entropy values at $0.1R_{200}$ and triangles at R_{500} . Solid lines represent least-squares fits to the simulated data. The data-points are results from Ponman et al. (2003), with the dashed line illustrating the self-similar slope ($S \propto T$), normalized to their 8 hottest clusters. The horizontal dotted line is the entropy floor, $S \sim 124 \text{ keV cm}^2$, from Lloyd-Davies et al. (2000).

in groups (Ponman et al. 1999). As shown previously (Muanwong et al. 2002; Kay et al. 2003), the *Non-radiative* model (open symbols) agrees well with the self-similar prediction ($S \propto T$), apart from at low temperatures where there is some scatter due to insufficient resolution in the core, while the *Radiative* model (filled symbols) is in reasonable agreement with the observations (the error-bars shown here are from Ponman et al. 2003).

We also show in this figure (triangles) results for a lower density contrast of 500, corresponding to $\sim 2/3R_{200}$. Again, our *Non-radiative* results agree well with the self-similar scaling but (allowing extrapolation) are around 40 per cent higher than the expected result when normalized to the hottest 8 clusters in the Ponman et al. sample (upper dashed line). Note however, that the *Radiative* results at R_{500} are higher than the observational data at all temper-

atures, but scale almost self-similarly ($S \propto T_X^{0.9}$). Cooling increases the entropy in clusters at all radii but in this case, disagrees with the observed slope. It is therefore apparent that cooling has been too efficient at generating excess entropy in the most massive clusters.

Fig. 2 illustrates the same relationships for our *Weak Feedback* and *Strong Feedback* runs. In the former case, we see that this model does a reasonable job at R_{500} , flatter than the self-similar relation, but the entropy at $0.1R_{200}$ is considerably lower than observed. In this model, the gas is not receiving enough entropy to escape from the inner (X-ray dominant) region of the halo, but the feedback is having a larger effect on the gas in lower-mass systems, even at R_{500} . (Note that reheated gas can lose some of its entropy through cooling.)

The *Strong Feedback* model, however, matches both relations very well. The increase in entropy allows the gas to escape to larger radii than previously, but the fate of this gas depends on the system size. In low-temperature systems, a significant fraction of hot gas gains enough entropy to escape the system entirely (Kay et al. 2003), resulting in an entropy excess that is shown here to be present even at large radii. This effect diminishes in higher-temperature systems, where the entropy level of the gas is sufficiently high that less material was able to escape.

3.2 Profiles

To illustrate more clearly the effects of cooling and heating on the entropy distribution of our clusters, we plot in Fig. 3 entropy profiles for two systems with $kT_X \sim 1$ & 3 keV respectively. At large radii in both cases, the *Non-Radiative* model has an entropy profile in reasonable agreement with the relation, $S \propto R^{1.1}$, as expected from spherical accretion shocks (Tozzi & Norman 2001). Both profiles flatten within ~ 10 per cent of R_{200} .

Cooling increases the entropy of the gas at all radii (by removing a significant fraction of gas over the age of the universe) except for in the very centre where the cooling time is very short, causing the entropy to drop sharply. These effects are more prominent in the smaller system, reflecting the increasing efficiency of cooling with decreasing halo mass.

The *Weak Feedback* profiles are similar to the *Radiative* profiles, except that they are lower in normalization. The feedback in this case is enough to prevent some gas from cooling but not to move it around in the cluster significantly. The *Strong feedback* model on the other hand shows greater differences. In the 1 keV system the entropy profile is above the *Radiative* profile out to $\sim 0.4R_{200}$, where they both become comparable. Feedback therefore has increased the core entropy over and above what is possible from cooling alone, by moving some of the hot gas (which did not cool in the *Radiative* model) to larger radii. In the hotter system, however, the *Strong Feedback* profile is slightly lower than the *Radiative* profile out to $\sim 0.2R_{200}$, where it decreases further, and at R_{500} is only slightly higher than the *Non-radiative* profile. In this system, a larger fraction of gas was retained by the halo due to its deeper gravitational potential well.

We note that the *Strong Feedback* profiles are a bit flatter than $R^{1.1}$ at R_{500} (supported by observations). Generally, systems above 1 keV have slopes between 0.8-0.9.

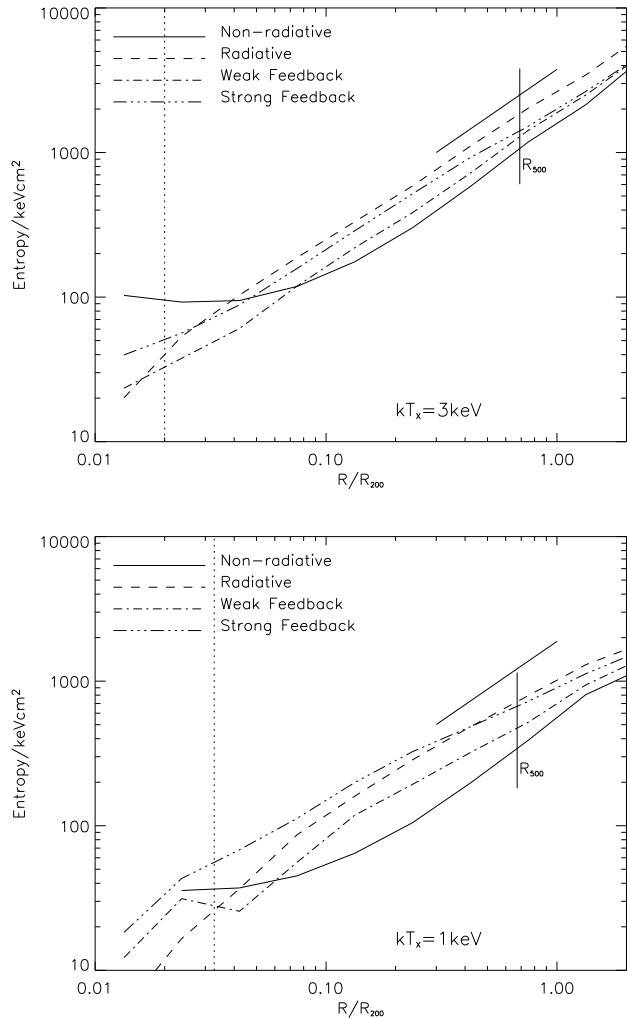


Figure 3. Entropy profiles for two haloes (top panel: $kT_X \sim 3$ keV and bottom panel: $kT_X \sim 1$ keV) at $z = 0$, from the *Non-radiative* simulation (solid curve), *Radiative* simulation (dashed curve), *Weak Feedback* simulation (dot-dashed curve) and the *Strong Feedback* simulation (triple-dot-dashed curve). The vertical dotted line marks the softening radius and the solid vertical line R_{500} . The solid diagonal line illustrates the predicted slope from spherical accretion shock models, $S \propto R^{1.1}$.

Whether this discrepancy is a problem with this model requires further investigation, but will greatly benefit from both larger simulations and a larger sample of high-quality cluster data.

4 SUMMARY

In this paper we used results from N -body/hydrodynamic simulations of the Λ CDM cosmology with various degrees of cooling and feedback, in order to understand the recent observational claim (Ponman et al. 2003; Pratt & Arnaud 2003) that the entropy of intracluster gas does not scale self-similarly with temperature out to at least R_{500} ($\sim 2/3R_{200}$). In particular, we compared our results to the entropy-temperature relation found by Ponman et al. at

$0.1R_{200}$ and at R_{500} , where both are found to be flatter ($S \propto T^{\sim 2/3}$) than the self-similar scaling ($S \propto T$). Our results can be summarized as follows.

- Non-radiative clusters scale self-similarly in the entropy-temperature plane to good approximation, both at $0.1R_{200}$ and at R_{500} . All but the largest clusters are observed to have an excess of entropy relative to the self-similar model at both radii.

- Radiative cooling raises the entropy in clusters at all radii. While this reproduces the entropy-temperature relation well at $0.1R_{200}$, it produces a relation that is too steep at R_{500} . In this case, the relation is almost self-similar, suggesting that clusters above a few keV have too much entropy compared to observations. This is due to the hot gas mass being too low at all radii.

- A feedback model in which gas receives a sufficient (1000 keV cm^2) amount of entropy results in excellent agreement with the observations at both radii. The reheated gas has enough entropy to escape the X-ray core but the fraction of material unable to leave the cluster (particularly at large radii) increases with system size, flattening the entropy-temperature relation. In detail, the entropy profiles are a bit flatter (at R_{500}) than suggested by observations, prompting future investigation into whether this discrepancy is significant.

We conclude that the entropy level required to match the observations is high, but supernovae are energetically capable, providing the energy is efficiently transported into lower density regions and contained within a small mass of gas. Alternatively, more energetic phenomena (hypernovae or Active Galactic Nuclei) may play a part.

ACKNOWLEDGEMENTS

We thank Peter Thomas for many helpful discussions and comments on the original manuscript, Trevor Ponman for providing useful comments and supplying data-points from the Birmingham-CfA Cluster Scaling Project and Volker Springel for making his code GADGET available to us. The simulations used in this paper were carried out using the Cosmology Machine at the Institute for Computational Cosmology, Durham as part of the Virgo Consortium programme of investigations into the formation of structure in the Universe. STK is supported by PPARC.

REFERENCES

Balogh M. L., Babul A., Patton D. R., 1999, MNRAS, 307, 463
 Balogh M. L., Pearce F. R., Bower R. G., Kay S. T., 2001, MNRAS, 326, 1228
 Bower R. G., 1997, MNRAS, 288, 355
 Bower R. G., Benson A. J., Lacey C. G., Baugh C. M., Cole S., Frenk C. S., 2001, MNRAS, 325, 497
 Brüggen M., Kaiser C. R., 2002, Nature, 418, 301
 Bryan G. L., 2000, ApJ, 544, L1
 Cole S., 1991, ApJ, 367, 45
 Cole S. et al., 2001, MNRAS, 326, 255
 Davé R., Katz N., Weinberg D. H., 2002, ApJ, 579, 23

Edge A. C., Stewart G. C., 1991, MNRAS, 252, 414
 Eke V. R., Navarro J. F., Frenk C. S., 1998, ApJ, 503, 569
 Evrard A. E., Henry J. P., 1991, ApJ, 383, 95
 Kaiser N., 1986, MNRAS, 222, 323
 Kaiser N., 1991, ApJ, 383, 104
 Kay S. T., Thomas P. A., Theuns T., 2003, MNRAS, 343, 608
 Knight P. A., Ponman T. J., 1997, MNRAS, 289, 955
 Kravtsov A. V., Yepes G., 2000, MNRAS, 318, 227
 Lloyd-Davies E. J., Ponman T. J., Cannon D. B., 2000, MNRAS, 315, 689
 Loewenstein M., 2000, ApJ, 532, 16
 Monaghan J. J., 1992, ARA&A, 30, 543
 Muanwong O., Thomas P. A., Kay S. T., Pearce F. R., Couchman H. M. P., 2001, MNRAS, 552, L27
 Muanwong O., Thomas P. A., Kay S. T., Pearce F. R., 2002, MNRAS, 336, 527
 Mushotzky R. F., Scharf C. A., 1997, ApJ, 482, L13
 Navarro J. F., Frenk C. S., White S. D. M., 1995, MNRAS, 275, 720
 Omma H., Binney J., Bryan G., Slyz A., 2003, MNRAS, submitted (astro-ph/0307471)
 Pearce F. R., Thomas P. A., Couchman H. M. P., Edge A. C., 2000, MNRAS, 317, 1029
 Ponman T. J., Cannon D. B., Navarro J. F., 1999, Nature, 397, 135
 Ponman T. J., Sanderson A. J. R., Finoguenov A., 2003, MNRAS, 343, 331
 Pratt G. W., Arnaud M., 2003, A&A, 408, 1
 Quilis V., Bower R. G., Balogh M. L., 2001, MNRAS, 328, 1091
 Raymond J. C., Smith B. W., 1977, ApJS, 35, 419
 Sanderson A. J. R., Ponman T. J., Finoguenov A., Lloyd-Davies E. J., Markevitch M., 2003, MNRAS, 340, 989
 Sanderson A. J. R., Ponman T. J., 2003, MNRAS, accepted (astro-ph/0307457)
 Springel V., Yoshida N., White S. D. M., 2001, New Astronomy, 6, 79
 Springel V., Hernquist L., 2002, MNRAS, 333, 649
 Strickland D. K., Stevens I. R., 2000, MNRAS, 314, 511
 Sutherland R. S., Dopita M. A., 1993, ApJS, 88, 253
 Tornatore L., Borgani S., Springel V., Matteucci F., Menci N., Murante G., 2003, MNRAS, 342, 1025
 Tozzi P., Norman C., 2001, ApJ, 546, 63
 Voit G. M., Bryan G. L., 2001, Nature, 414, 425
 Voit G. M., Bryan G. L., Balogh M. L., Bower R. G., 2002, ApJ, 576, 601
 Voit G. M., Balogh M. L., Bower R. G., Lacey C. G., Bryan G. L., 2003, ApJ, 593, 272
 White S. D. M., Rees M. J., 1978, MNRAS, 183, 341
 Wu K. K. S., Fabian A. C., Nulsen P. E. J., 2000, MNRAS, 318, 889
 Wu X.-P., Xue Y.-J., 2002, ApJ, 569, 112